Explosive reconnection of the double tearing mode in relativistic plasmas

Application to the Crab

Jérôme Pétri[1] Hubert Baty[1] Makoto Takamoto[2,*] Seiji Zenitani[3]

[1]Observatoire astronomique de Strasbourg, Université de Strasbourg, France.

[2]Max-Planck Institute for Nuclear Physics, 69117 Heidelberg, Germany. (* now in Japan)

[3]National Astronomical Observatory of Japan, Tokyo 181-8588, Japan.

Summary

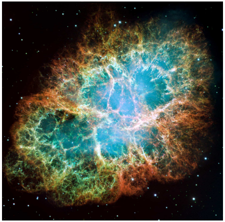

Figure : *The Crab nebula.*

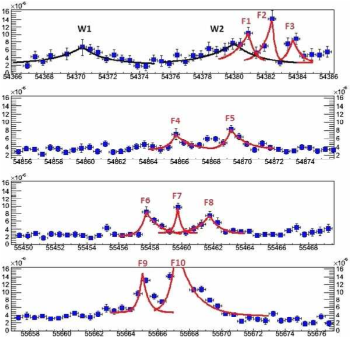

Figure : *Temporal evolution of the Crab flares seen in gamma-rays (Striani et al., 2013).*

- unexpected fluctuations in the gamma-ray flux
- increase by a factor 10
- variations on a day scale
  - strong flares (F) lasting one day
  - weak waves (W) lasting one or two weeks
- short but powerful flares (E$\approx 10^{34}$ J)
- isotropic power = sizeable fraction of the spin-down luminosity

Special features

- only seen in gamma-rays (100 MeV-1 GeV)
- peak emission around 400 MeV
- no counterpart in X-rays or VHE (Weisskopf et al., 2013)
- a few events/year

The April 2011 event (Buehler et al., 2012)

- time scales of 20 min
- rising time of 8 hours
- fit of the spectral evolution
  - power law $\Gamma = 1.27 \pm 0.12$
  - with exponential cut-off E_c
  - synchrotron flux > 100 MeV

$$L_{\mathrm{100MeV}} \propto E_c^{3.42\pm0.86}$$

  - at the peak $E_c \approx 375$ MeV
  - $L_{\mathrm{100MeV}} \approx 4 \times 10^{29}$ W$\approx 0.01\, L_{\mathrm{sd}}$

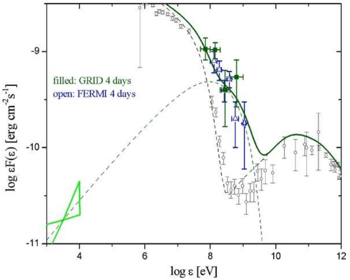

Figure : *Spectra of the Crab flare seen in gamma-rays (Vittorini et al., 2011).*

The pulsar linked to its surrounding nebula

- the pulsar and its magnetosphere, source of *relativistic* $e^{\pm}$ *pairs* $r_{\rm L} = 10^6$ m.
- the cold ultra-relativistic wind streaming to the nebula.
- the shocked wind composed of particles heated after crossing the *MHD shock*, $r_{\rm ts} = 3 \times 10^{15}$ m$= 0.1$ pc $\Rightarrow$ *main source of radiation* observed in radio, optics, X-rays and gamma-rays.
- the supernova remnant.
- the interstellar medium.

Figure : *Link between the pulsar and its surrounding nebula.*

Supernova remnant and nebula

The pulsar linked to its surrounding nebula

- the pulsar and its magnetosphere, source of *relativistic e$^\pm$ pairs* $r_{\rm L} = 10^6$ m.
- the cold ultra-relativistic wind streaming to the nebula.
- the shocked wind composed of particles heated after crossing the *MHD shock*, $r_{\rm ts} = 3 \times 10^{15}$ m$= 0.1$ pc $\Rightarrow$ *main source of radiation* observed in radio, optics, X-rays and gamma-rays.
- the supernova remnant.
- the interstellar medium.

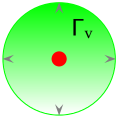

Figure : *Link between the pulsar and its surrounding nebula.*

Supernova remnant and nebula

The pulsar linked to its surrounding nebula

- the pulsar and its magnetosphere, source of *relativistic* $e^{\pm}$ *pairs* $r_{\mathrm{L}} = 10^6$ m.
- the cold ultra-relativistic wind streaming to the nebula.
- the shocked wind composed of particles heated after crossing the *MHD shock*, $r_{\mathrm{ts}} = 3 \times 10^{15}$ m$=$ 0.1 pc $\Rightarrow$ *main source of radiation* observed in radio, optics, X-rays and gamma-rays.
- the supernova remnant.
- the interstellar medium.

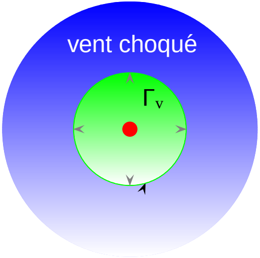

Figure : *Link between the pulsar and its surrounding nebula.*

Supernova remnant and nebula

The pulsar linked to its surrounding nebula

- the pulsar and its magnetosphere, source of *relativistic $e^{\pm}$ pairs* $r_{\rm L} = 10^6$ m.
- the cold ultra-relativistic wind streaming to the nebula.
- the shocked wind composed of particles heated after crossing the *MHD shock*, $r_{\rm ts} = 3 \times 10^{15}$ m$= 0.1$ pc $\Rightarrow$ *main source of radiation* observed in radio, optics, X-rays and gamma-rays.
- the supernova remnant.
- the interstellar medium.

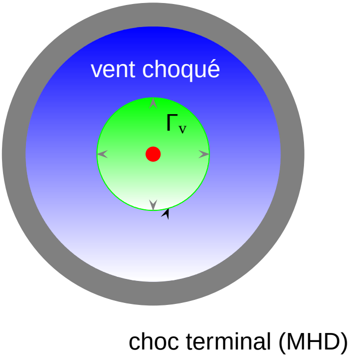

Figure : *Link between the pulsar and its surrounding nebula.*

The pulsar linked to its surrounding nebula

- the pulsar and its magnetosphere, source of *relativistic* $e^{\pm}$ *pairs* $r_{\rm L} = 10^6$ m.
- the cold ultra-relativistic wind streaming to the nebula.
- the shocked wind composed of particles heated after crossing the *MHD shock*, $r_{\rm ts} = 3 \times 10^{15}$ m$= 0.1$ pc $\Rightarrow$ *main source of radiation* observed in radio, optics, X-rays and gamma-rays.
- the supernova remnant.
- the interstellar medium.

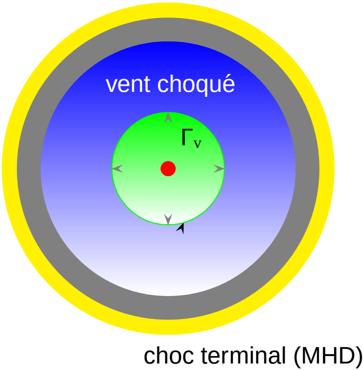

Figure : *Link between the pulsar and its surrounding nebula.*

Supernova remnant and nebula

The pulsar linked to its surrounding nebula

- the pulsar and its magnetosphere, source of *relativistic $e^{\pm}$ pairs* $r_{\rm L} = 10^6$ m.
- the cold ultra-relativistic wind streaming to the nebula.
- the shocked wind composed of particles heated after crossing the *MHD shock*, $r_{\rm ts} = 3 \times 10^{15}$ m$=$ 0.1 pc $\Rightarrow$ *main source of radiation* observed in radio, optics, X-rays and gamma-rays.
- the supernova remnant.
- the interstellar medium.

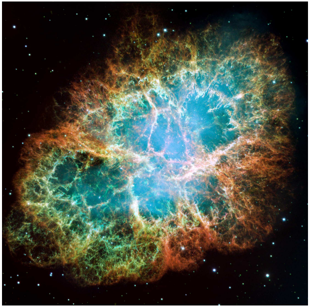

Figure : *The Crab pulsar/nebula.*

Simple estimates

Comparing the time scales

- too long for the Crab pulsar (33 ms)
- too short for the nebula evolution (years)
- size of emitting region, $L_f \approx c\,\Delta t \approx 10^{-3}$ pc

Possible locations

- within the striped wind $r_L < R_f < r_S$.
- at the termination shock $R_f = r_S$.
- within the nebula $R_f > r_S$.

Near the star:
a magnetic dipole

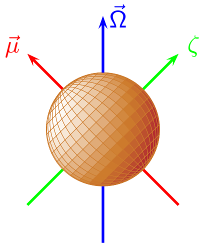

At large distances:

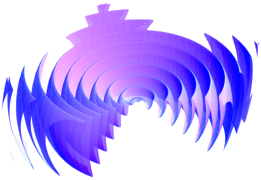

Figure : *striped wind (Bogovalov, 1999).*

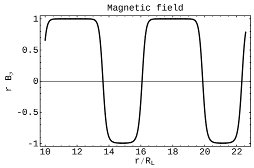

Figure : *3D view of the current sheet.*

- $\vec{\Omega}$: rotation axis
- χ: magnetic axis inclination with respect to $\vec{\Omega}$
- ζ: line of sight inclination with respect to $\vec{\Omega}$

$$\left.\begin{array}{l}\text{- hot and magnetized plasma in the sheet}\\ \text{- relativistic beaming } \Gamma_{\rm vent} \gg 1\end{array}\right\} \Rightarrow \text{pulsed emission}$$

- timescale of reconnection $\tau \approx \sqrt{\tau_A \, \tau_D}$
  as in classical MHD
  τ_A Alfven timescale
  τ_D diffusion timescale
- outflow not relativistic
- reconnection rate to slow for the flares

$\Rightarrow$ tearing instability unable to explain fast rising time

- the answer: double tearing mode (Baty et al., 2013)

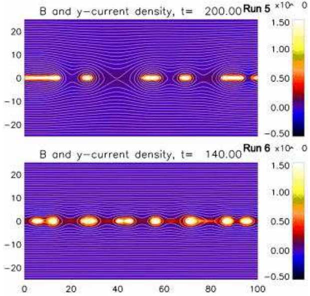

Figure : *Relativistic pair plasma reconnection (Hesse & Zenitani, 2007).*

Numerical setup

Double Harris current sheet

$$B_x = B_0\,(1 + \tanh(\frac{y - y_0}{L}) - \tanh(\frac{y + y_0}{L}))$$

- width of one current sheet, $L = 1$
- separation $2\,y_0 = 6\,L$
- uniform temperature $T = 1$
- normalization: magnetic field $B^2 = 2$ and density $\rho = 1$
- specific heat ratio $\Gamma = 4/3$
- Alfven speed

$$v_A = c\sqrt{\frac{\sigma}{\sigma + 1}}$$

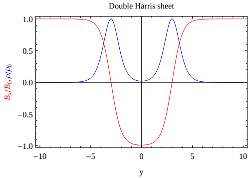

Figure : *The two current sheets in the simulations.*

Two free parameters

- magnetization σ
- Lundquist number $S = L\,c/\eta$

Simulation example

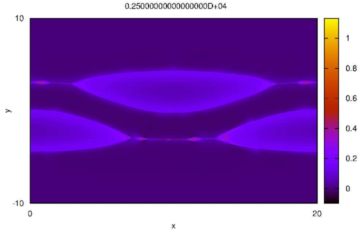

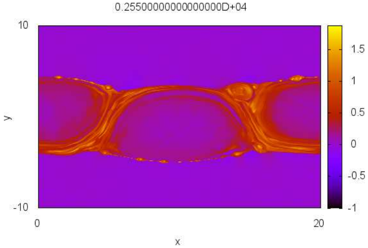

Simulation example: four stages

1. linear evolution of the DTM as an antisymmetric pattern
2. saturation: Rutherford regime (maximal size of the islands with diffusion)
3. secondary instability: fast non-linear evolution
4. relaxation to the final state: magnetic field dissipated into bulk motion and particle thermalization

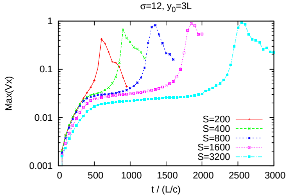

Figure : *Maximum flow velocity V_x with $\sigma = 12$.*

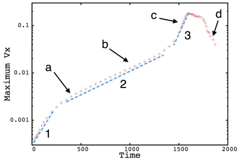

Figure : *The four phases in the DTM (Baty et al., 2013).*

Time scales

- observational constrain $\Delta T \lesssim \tau_r \approx 10$ hr $\Rightarrow \Gamma \lesssim 150$
- consistent with $\Gamma \approx 20 - 50$ from Pétri & Kirk (2005)

Energetics

- energy release in a flare 10^{34} J
- local magnetic field in the flare around 2 T
- wave nature of the striped wind implies emission at $r \approx 50\, r_{\rm L}$.
- luminosity according to $L = \mathcal{D}^4\, L'$
- in agreement with the 2011 flare $L_{>100\,{\rm MeV}} \propto \varepsilon_c^{3.42\pm0.86}$ (Buehler et al., 2012)

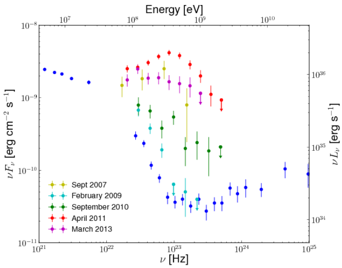

Figure : *Spectra of several Crab flares.*

Flares in the nebula

Conclusions

- double tearing instability is good candidate to explain short and powerful gamma-ray flares in strongly magnetized plasmas
- orders of magnitude in agreement with Crab flares
- striped wind is a natural place where to expect double tearing
- parameters for the pulsar wind consistent with independent estimates (pulsed radiation)

Perspectives

- effect of multiple current sheets (multiple tearing mode)
- PIC simulations including particle acceleration
- feedback of radiation reaction: synchrotron/inverse Compton

Contribution of multipolar fields to radio and high-energy emission of pulsars

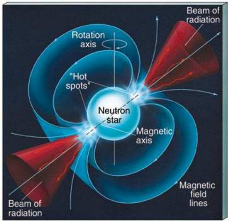

Schematic view of a pulsar.

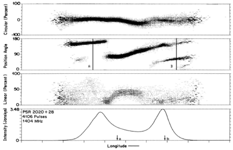

Example of radio-polarisation.

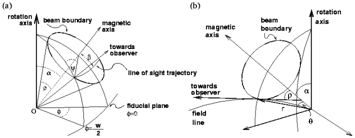

Taken from "Handbook of Pulsar Astronomy" by Lorimer & Kramer

A polar cap.

Taken from "Handbook of Pulsar Astronomy" by Lorimer & Kramer

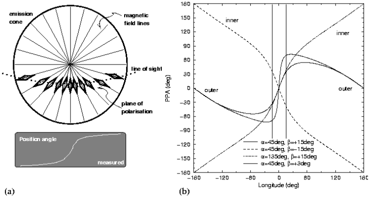

Rotating vector model and explanation for polarisation.

http://amwdb.u-strasbg.fr/HighEnergy/spip.php?article271

Baty H., Petri J., Zenitani S., 2013, MNRAS, 436, L20

Bogovalov S. V., 1999, A&A, 349, 1017

Buehler R. et al., 2012, ApJ, 749, 26

Hesse M., Zenitani S., 2007, Physics of Plasmas, 14, 112102

Pétri J., Kirk J. G., 2005, ApJL, 627, L37

Striani E. et al., 2013, ApJ, 765, 52

Vittorini V. et al., 2011, ApJL, 732, L22

Weisskopf M. C. et al., 2013, ApJ, 765, 56